

Monte Carlo Modeling of L3 Detectors in High Time Resolution Applications.

Simon Tulloch

*Isaac Newton Group, Apartado 321
Santa Cruz de La Palma, Canarias
38700, SPAIN*

Abstract. I have developed an IDL simulation of an electron multiplying L3 (low light level) technology CCD that includes the effects of clock induced charge and multiplication noise. This model allows observers interested in obtaining high time resolution photometry and spectroscopy of faint sources to compare more easily the gains in performance that can be expected by switching to an L3 detector. The model has been used to generate synthetic image sequences of stars and emission lines. The stellar images are analysed to show how the measured centroid noise of the star varies with the source brightness. In the case of the synthetic spectra the analysis determines how the SNR of a Gaussian line fit varies with the source brightness. In order to provide points of reference, the results are compared with both an ideal detector and a conventional CCD with various levels of read noise. The results show how closely an L3 CCD can approach to an ideal detector in various observing regimes. The performance of an L3 detector in photon counting mode is also investigated.

Keywords: CCD Photon Counting Electron Multiplying L3

PACS: 07.07.Df, 95.55.Aq

INTRODUCTION TO L3 TECHNOLOGY CCDS

The operation of conventional CCDs usually requires a trade off between read noise and frame rate. L3 technology allows these two parameters to be decoupled and it is possible to attain sub-electron read-noise at pixel rates up to 15 MHz. In high frame rate applications they are therefore an attractive choice. L3 CCDs have some operational features, however, that can restrict their performance in certain regimes. It is important that any potential user be aware of these limitations, which are detailed in this section. The output of any CCD consists of a MOSFET transistor to convert the pixel photo-charge into an output voltage. This voltage is further amplified and digitized off-chip. Any well designed camera system will be limited in its performance by the noise voltage of this on-chip amplifier. Recent advances have reduced this noise to the level of about $2e^-$ RMS at pixel rates of 100 kHz, however, at pixel rates of 10 MHz it can reach $20e^-$, seriously reducing the SNR of observations. L3 technology uses an avalanche multiplication process to boost the pixel photo-charge prior to its reaching this output amplifier. The charge amplification is sufficiently great that even in the case of a single photo-electron of input the output signal is large enough to render the amplifier noise contribution negligible. Single photo-electrons can therefore be easily detected. This extreme sensitivity is demonstrated in Fig. 1 where 'photon diffraction' from a faintly illuminated pin hole is visible. The left part

of the image shows a single frame, the right part shows the sum of 50 such frames after they have been thresholded and stacked (i.e. photon counted).

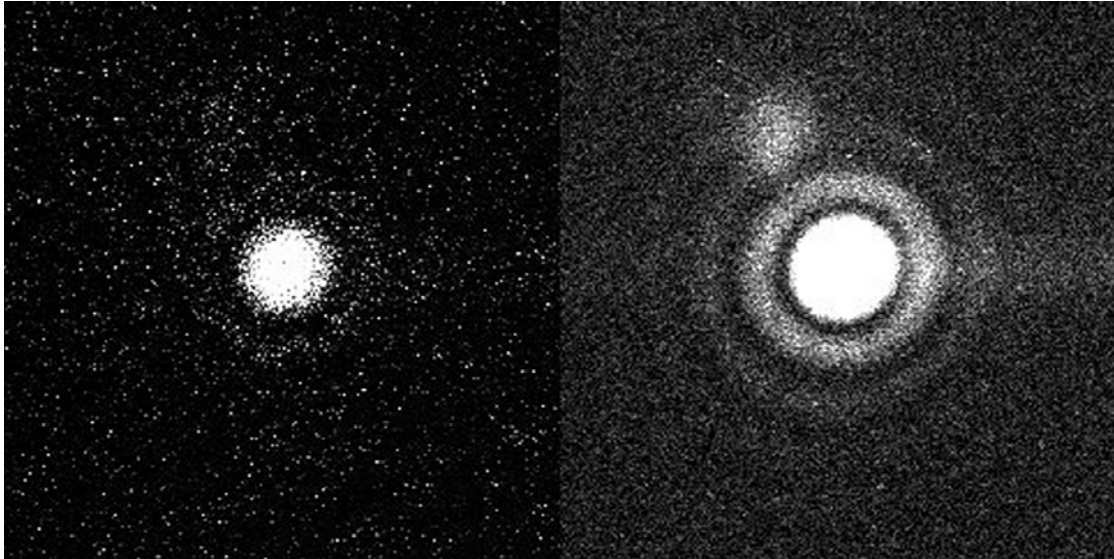


FIGURE 1. Photon Diffraction observed with an L3 CCD

Multiplication Noise

The multiplication process takes place in a 520 stage avalanche (or multiplication) register. The gain in each stage is quite low, just a few percent. The actual gain level can be controlled by varying the amplitude of a multiplication clock. The statistics of the multiplication process give a rather non-intuitive signal distribution at the CCD output ². The effect is that a large range of input signal levels can produce the same output signal from the avalanche register. This constitutes an additional noise source, called multiplication noise. Further analysis reveals that the effect of multiplication noise is to reduce the SNR of observations by $\sqrt{2}$ in the photon noise limited regime. This is statistically equivalent to saying that the detector loses a factor of 2 in quantum efficiency. In the detector noise limited regime (low signal levels), however, this loss will be more than compensated for by the negligible read noise of the L3 CCD.

Clock Induced Charge (CIC)

The clock transitions within the image area of a CCD can produce spurious electrons in the device, an effect known as clock induced charge (CIC). This charge generation happens as a pixel transfers from the inverted to the non-inverted state ^{3,4}, and is caused by holes being accelerated into the silicon bulk where they produce charge carriers through impact ionization. The effect can be reduced by operating the CCD in non-inverted mode but this has the effect of increasing the dark current and therefore

requires operation at reduced temperature. CIC is not normally noticed in a conventional CCD since its effect is swamped by read noise, but in the L3 device these extra spurious electrons are clearly visible and are an important noise source. The level of the noise is proportional to the number of rows in the CCD i.e. the number of vertical transfers through which a pixel has traveled. The manufacturers claim a minimum level of 3×10^{-6} electrons per pixel per transfer⁵ which corresponds to $0.006e^-$ per pixel per frame for a device with 2K rows. L3 cameras operated at the Isaac Newton Group of Telescopes (ING) have shown a CIC of 1.5×10^{-5} electrons per pixel per transfer.

CCD Noise Characteristics

The graph shown in Figure 2. was obtained from a series of flat fields taken with an L3 camera at several different multiplication levels (which were varied by tuning the amplitude of a multiplication clock). The solid black line shows the result that would be obtained from a conventional detector at high signal levels i.e. variance = mean of signal. Compare this with the L3 result where the variance = 2 x mean of signal. This graph clearly shows the effect of the multiplication noise.

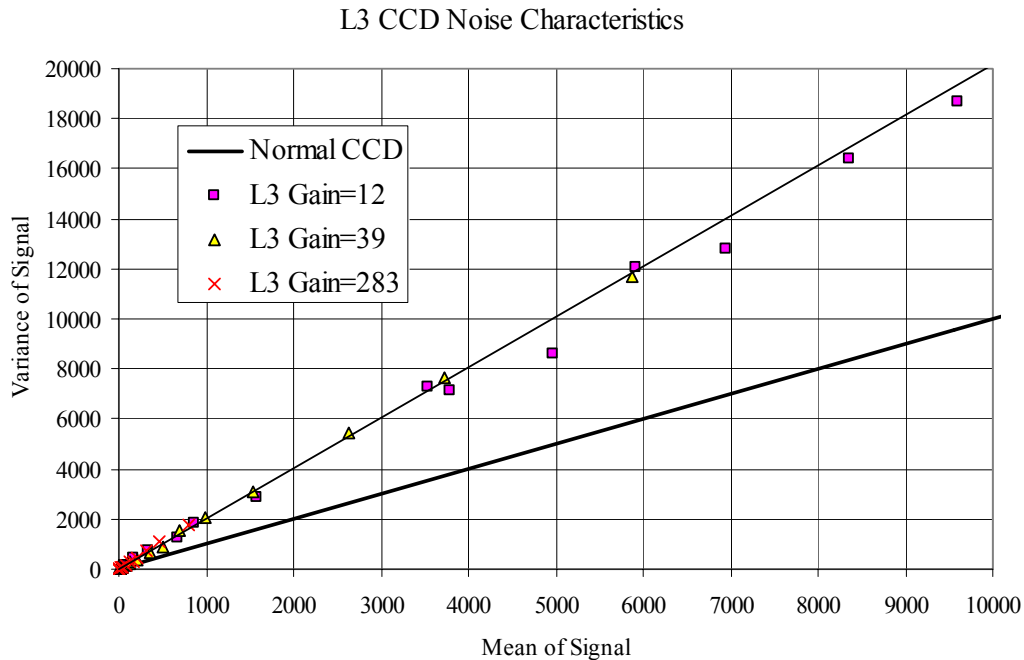


FIGURE 2. Photon transfer characteristics of L3 compared to a conventional CCD

With regard to read-noise generated in the output amplifier, in the case of L3 this is practically insignificant if the system is well set up. For a conventional CCD the noise levels presented in Table 1 are typical¹:

TABLE1. Conventional CCD Noise Levels		
Pixel Rate	Equivalent Frame Rate (1000x100 pixel window)	RMS read noise e-
100 kHz	1 Hz	2.2
330 kHz	3 Hz	3
1 MHz	10 Hz	5
5 MHz	50 Hz	10
10 MHz	100 Hz	20

These values are used later when comparing L3 and conventional CCDs. The window size of 1000 x 100 pixels is taken as a typical value for spectroscopy applications.

Interpreting L3 Data

L3 images can be interpreted and analysed in the same way as a conventional image i.e. the digitized pixel value can be multiplied by the overall system sensitivity to yield the corresponding input illumination. This mode will from now on be referred to as Proportional Mode. The ability to resolve individual photons raises the interesting possibility of applying photon counting to the images. Here a threshold is applied to an input image and a pixel value is interpreted as being either a 1 or a 0. A large number of images will then need to be thresholded and added in this way in order to yield a useful SNR. The input images must necessarily have a low illumination in order to avoid coincidence losses. The advantage of Photon Counting Mode is that the multiplication noise is overcome and once again the variance = mean of signal. In order to extract the maximum SNR from an image one can even imagine separate parts of the same image (or sequence of images) being subjected to these two different forms of analysis.

Some Actual L3 Camera Results

Several L3 cameras have already been operated at the ING. The first was a cryogenically cooled 128 x 128 pixel E2V CCD60. This was used on the 4.2m William Herschel Telescope to directly observe the variations in the Crab Nebula Pulsar without resorting to phase folding. A sequence of images covering 3 pulsar periods is shown in Figure 3.

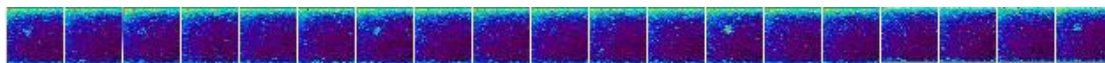


FIGURE 3. Sequence of L3 observations of the Crab Nebula Pulsar (180 frames s⁻¹)

A CCD60 has subsequently been used at the ING for wavefront sensing in the GLAS adaptive optics (AO) system. A larger 1k x 1k pixel frame transfer E2V CCD201 has since been used for spectroscopy at frames rates up to about 2Hz. An example emission spectrum is shown in Figure 4. This image also demonstrates CIC

which appears as a peppering of bright pixels in the background, each corresponding to a single electron. The mean CIC level in this image is $0.03e^-$ per pixel.

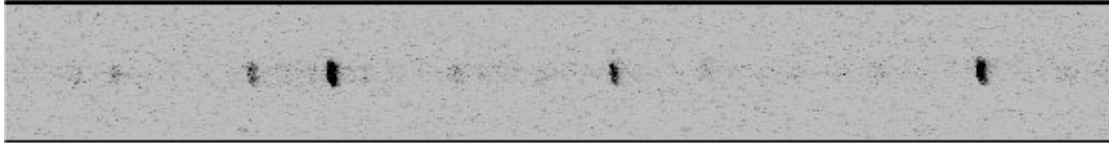


FIGURE 4. An example spectrum from an L3 camera. CIC visible in background

MONTE CARLO MODELING OF AN L3 CCD

A model of an L3 CCD was developed using the Interactive Data Language (IDL). The model included the effects of Poissonian noise in the input images, multiplication noise, the small contribution of Gaussian noise in the output amplifier and CIC at two different levels corresponding to what we have obtained in the lab and what the manufacturers quote as the achievable performance. Dark current and sky background were not included. QE was also not included since this is uniformly high for all the detectors; the model in fact dealt in units of photo-electrons rather than photons. For comparison, a second model was developed of a conventional CCD operated at various read-out speeds with their corresponding noise levels. The models were used to compare performance in two applications: wavefront sensing and rapid spectroscopy. In the former, a large sample of synthetic guide star images of varying brightness were generated to assess the centroiding noise achievable and therefore show in which regimes an L3 device may provide better performance when part of an adaptive optics system. For the latter application, the same set of synthetic stars was interpreted as being an emission line and the model was used to fit a Gaussian profile to this line. The goodness of this fit at various signal levels then showed where an L3 device offered an advantage over a conventional CCD. For the centroiding investigation Proportional Mode analysis of the L3 images was used since Photon Counting cannot be used at the high frame rates needed for wavefront sensing. For the spectroscopy investigation both Proportional mode and Photon Counting mode were considered. The model assumed that the CCD in question had 2048 rows, even though only a small windowed section was actually digitized. The only implication of this was the level of CIC that was modeled; the minimum level of CIC quoted by the manufacturer had units of e^- per line transfer (i.e. total number of CCD image rows).

Generation of Synthetic Images

The synthetic images were generated in stacks of 5000. Approximately 30 stacks were created for each detector at exposure levels ranging from 0.05 to 20000 photo-electrons frame^{-1} (integrated brightness). A bias stack was also created for each detector. All images within a stack had the same mean brightness modulated by a Poissonian factor to give the correct photon noise.

The images had the following characteristics:

Frame size : 16x16 pixels.

Image size : circular spot of Gaussian profile FWHM =3 pixels, offset from centre of frame by 0.5 pixel in X and 1 pixel in Y.

The detector models had the following characteristics:

- 1) Conventional CCD with $2.2e^-$ read noise (typical at 100 kPix s^{-1})
- 2) Conventional CCD with $3e^-$ read noise (typical at 330 kPix s^{-1})
- 3) Conventional CCD with $5e^-$ read noise (typical at 1 MPix s^{-1})
- 4) Conventional CCD with $10e^-$ read noise (typical at 5 MPix s^{-1})
- 5) Conventional CCD with $20e^-$ read noise (typical at 10 MPix s^{-1})
- 6) L3 CCD with $30e^-$ read noise, L3 gain of 1000, $\text{CIC}=0.03e^- \text{ pixel}^{-1} \text{ readout}^{-1}$
- 7) L3 CCD with $30e^-$ read noise, L3 gain of 1000, $\text{CIC}=0.006e^- \text{ pixel}^{-1} \text{ readout}^{-1}$

[NOTE. The L3 read noise of $30e^-$ is typical at the highest frame rates achievable. It is the noise at the *output* of the CCD, after the photo-electrons have been multiplied. Its level referenced to the image area of the CCD is therefore $0.03e^-$ i.e. divided by the L3 multiplication factor. This should not be confused with the level of CIC used for one of the models.]

Analysis of the Images

The analysis path of the synthetic image is shown in Figure 5. The L3 images were analysed both in Proportional Mode and Photon Counting Mode. In the latter it was necessary to sum the thresholded images prior to Gaussian line fitting. Two different summing or 'blocking' values were investigated: 10 and 100.

RESULTS: APPLICATION TO WFS

A typical wavefront sensing application requires a small window (6x6 pixels would be usual) to be analysed using a weighted centre of gravity algorithm using a threshold to exclude pixels that contain only noise. Frame rates of at least 100Hz are required for useful atmospheric correction. In some extreme AO applications, frame rates of 3kHz are proposed. In this analysis a 3σ threshold was used and a pixel weighting = signal to the power of 1.5. The window position was chosen so that the synthetic guide star image was offset by 0.5 pixels from the centre. This was important since there is tendency for the centre of gravity algorithm to give a result that drifts towards the centre of the window as the signal falls in intensity and this can give falsely low values for the centroiding noise. The algorithm was applied to each of the stars in each

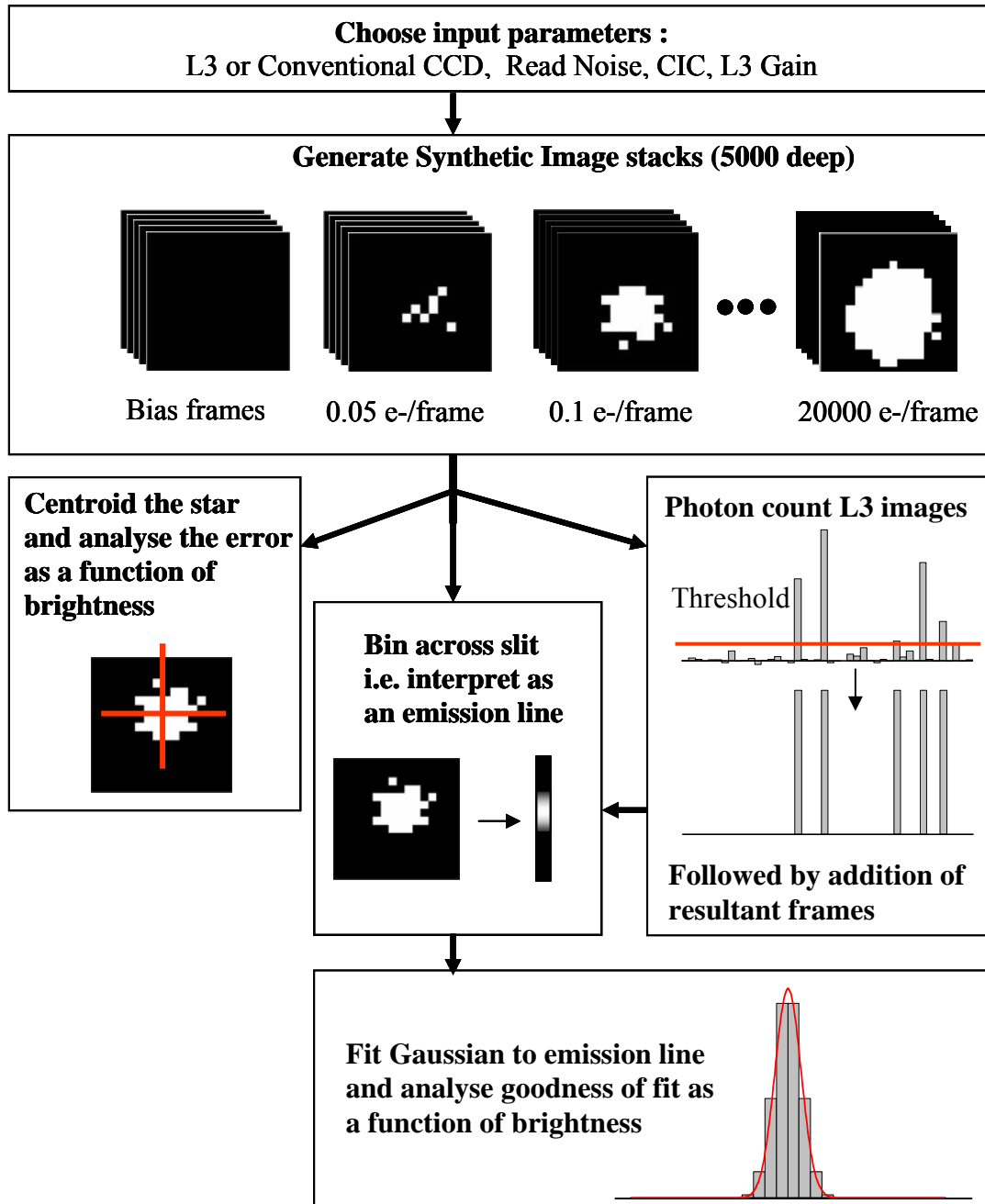


FIGURE 5. Analysis path of the study

image stack and the mean and standard deviation of the resultant centroid value was recorded and then plotted as a function of the star's intensity. The mean centroid value was also recorded and checked manually to ensure that the algorithm was functioning correctly. The standard deviations are plotted later in this section. As a check of the analysis procedure some extra stacks of 'ideal' guide star images were generated i.e. images that contained only Poissonian noise and no CIC or read noise. It was then

confirmed that the centroid noise measured on these ideal images agreed well with the established theoretical minimum value ⁶ shown in equation 1.

$$\sigma_{MIN} = \frac{\sigma_{SPOT}}{\sqrt{N_{PHOTONS}}} \quad (1) \quad \text{where} \quad \sigma_{ISPOT} = \frac{FWHM_{SPOT}}{2\sqrt{2\ln 2}}$$

The centroiding error predicted by the model was in fact 10-15% higher than the theoretical value. As a further experiment, pixel weighting and threshold values were varied. This showed that the values quoted above were optimum. The threshold value of 3σ was found to be a good choice since lower values caused the centroid to drift in the direction of the window centre. The weighting of signal to the power of 1.5 was also found to be a good choice for the same reason.

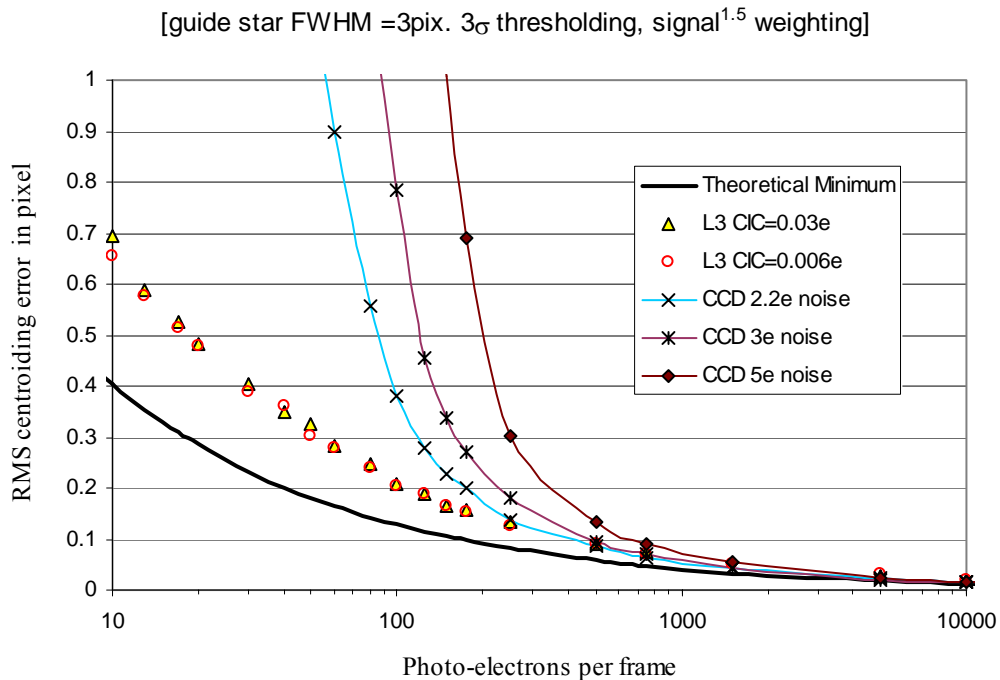


FIGURE 6. Centroiding error as a function of guide star intensity (low end)

The results are interesting and show a clear advantage to using an L3 detector if the integrated guide star intensity is below about 200e⁻ per frame. Surprisingly, the CIC only slightly degrades the centroiding accuracy. At the high exposure end, re-plotted in Figure 7, the effects of the multiplication noise in the L3 detector becomes apparent and a conventional CCD, even one with a read noise of 5e⁻, produces less noisy centroids.

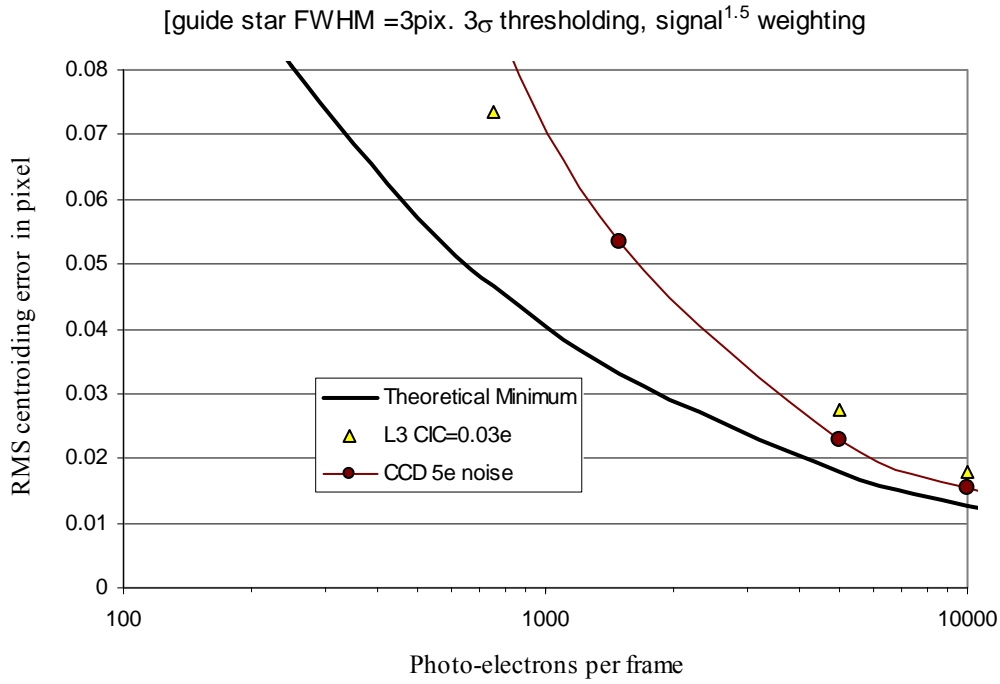


FIGURE 7. Centroiding error as a function of guide star intensity (high end)

RESULTS: APPLICATION TO RAPID SPECTROSCOPY

The same image stacks were used for this second part of the study although they were interpreted as being spectral emission lines rather than guide stars. The aim here was to show how well a spectral line could be measured using an L3 compared to a conventional CCD, as a function of the line brightness. The images were first binned by a factor of 7, a factor high enough to include almost all the signal in a single row and a value typical in real observations. This binning was done ‘off chip’. This 1-D image was then padded at each end with similarly binned bias pixels to give a resultant 30 pixel long spectrum with an emission line close to its centre. Two functions were then fitted to this image: a constant and a Gaussian. The goodness of these two fits was then used to calculate the SNR of the observation using the standard technique shown in equation 2.

$$SNR = \sqrt{\chi_{CONST}^2 - \chi_{GAUSS}^2} \quad (2)$$

The line fitting used was an optimal mean procedure that had fixed parameter values for the line centre and width. The procedure took two input parameter vectors, the first contained the pixel values, the second was an array of measurement errors. The measurement errors were calculated by adding in quadrature the bias noise and the photon noise. The bias noise was measured from the bias image stack after it had been binned by the same factor as the spectral line (in the case of the Photon Counting mode these bias pixels had also to be passed through the thresholding process). The

photon noise was calculated theoretically from the known line profile. In the case of the L3 images the multiplication noise factor also had to be included in the photon noise calculation. The line fitting procedure thus had *a priori* knowledge of all the parameters of the line that it was trying to detect in the noisy images.

In addition the proportional analysis described above, the L3 images were also passed through a photon counting analysis. Here an extra stage was introduced where the images were thresholded and converted to units of photons prior to the binning operation. Blocks of 10 and 100 images were then added together before being passed on to the Gaussian line fitting procedure. Since photon counting only works on faint sources where coincidence losses are low, this ‘blocking’ is required to yield an analyzable image. It means that the effective frame rate (rate of analyzable spectra) is much lower than the actual frame rate by at least an order of magnitude.

Proportional analysis of conventional and L3 CCD images

The SNR ratios of the Gaussian line fits were plotted against integrated line brightness, expressed in photo-electrons s^{-1} , for frame rates of 1, 10 and 100Hz. The SNR of the L3 detectors are independent of frame rate: as mentioned earlier the read noise is decoupled from the readout speed. In the case of the conventional CCD the noise rises with frame rate. The graph for each spectral frame rate therefore contains the same L3 data suitably re-scaled along the horizontal axis but with a different data set for the conventional detectors. For example, in the 1 Hz frame rate graph the L3 performance was compared with a conventional detector of $2.2e^{-}$ read noise¹ but for the 100Hz frame rate graph it was compared with a conventional detector of $20e^{-}$ read noise. These are the noise levels expected (see table 1) if we assume the detector has a 1000×100 pixel readout window; a realistic size for actual spectroscopic observations. An additional graph (Figure 8) is also included with the x-axis labeled in photons per frame rather than photons per second at a specified frame rate. As can be seen from the graphs, the L3 detector only becomes competitive at very high frame rates and then only within the low signal domain. If we are simply trying to detect the presence of an emission line then L3 can do it with about half as many photons as the best conventional detector. If the line is brighter then the multiplication noise of the L3 detector will be higher and this tips the balance in favor of a conventional detector, especially if pixel rates are low.

Photon Counting Analysis of L3 CCD images

The maximum speed at which an L3 detector can read out a 1000×100 pixel image is around 100Hz. If we assume that between 10 and 100 photon counted frames must be blocked (added) to yield a measurable spectra then the maximum spectral frame rate will be about 10Hz. The photon counting performance is also included in Figures 9 and 10. In Figure 9 the *spectral* rate was 1Hz and the photon counting frame rate 100Hz so the blocking factor was 100. In Figure 10 the spectral rate of 10Hz required a smaller blocking factor of only 10 frames. The latter figure clearly shows the effect of coincidence losses. The disappointing performance in this mode is understandable

if we consider the CIC. This noise source is effectively multiplied by the blocking factor. This constrains performance at the low end whilst at the higher end we are limited by coincidence loss. In between we have a narrow region where some minor gains are possible.

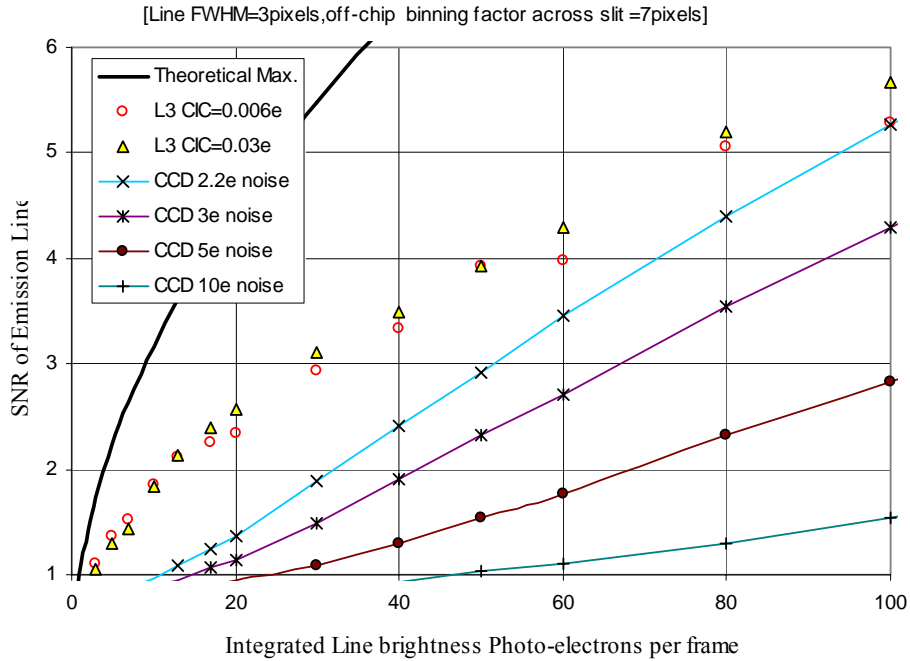


FIGURE 8. Emission line detection : conventional versus L3 CCDs

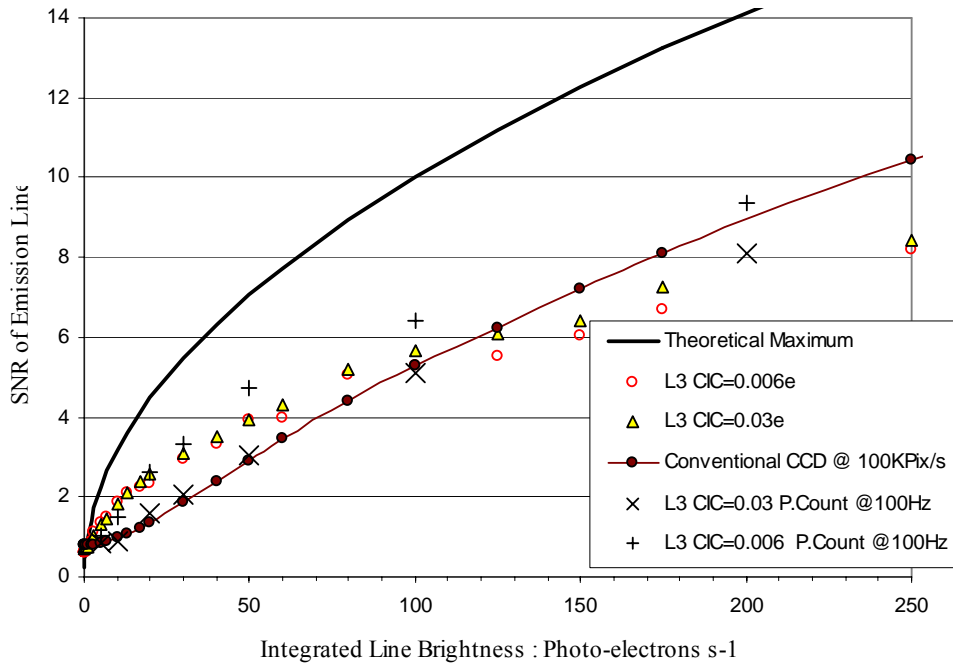


FIGURE 9. Emission line measurement : 1 Spectra s⁻¹ data rate (photon counting also shown)

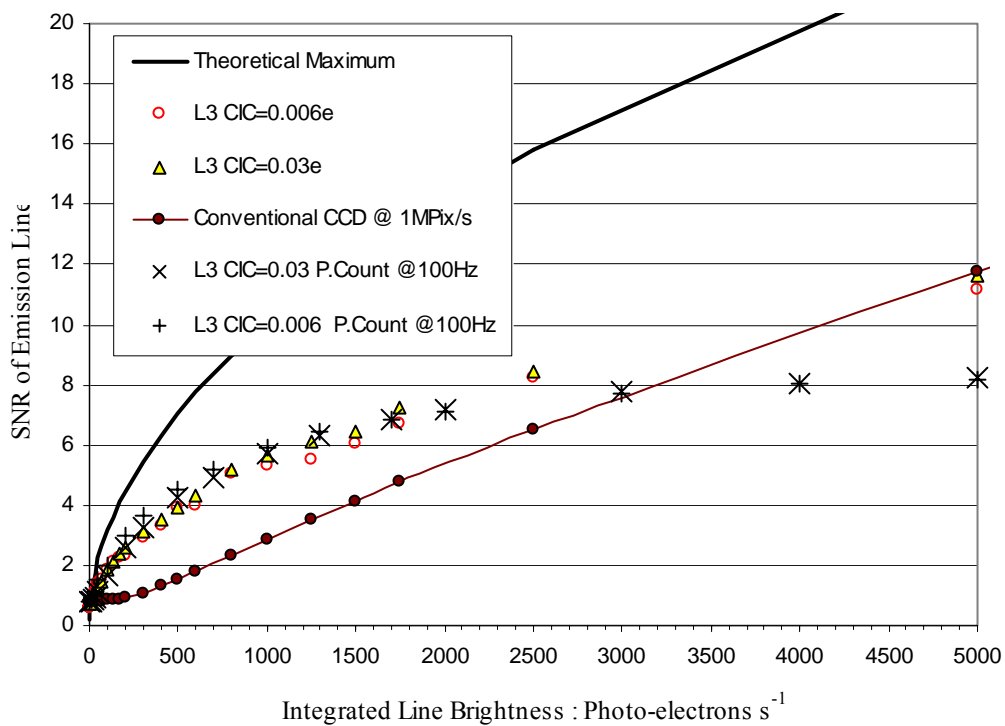


FIGURE 10. Emission line measurement: 10 Spectra s^{-1} data rate (photon counting also shown)

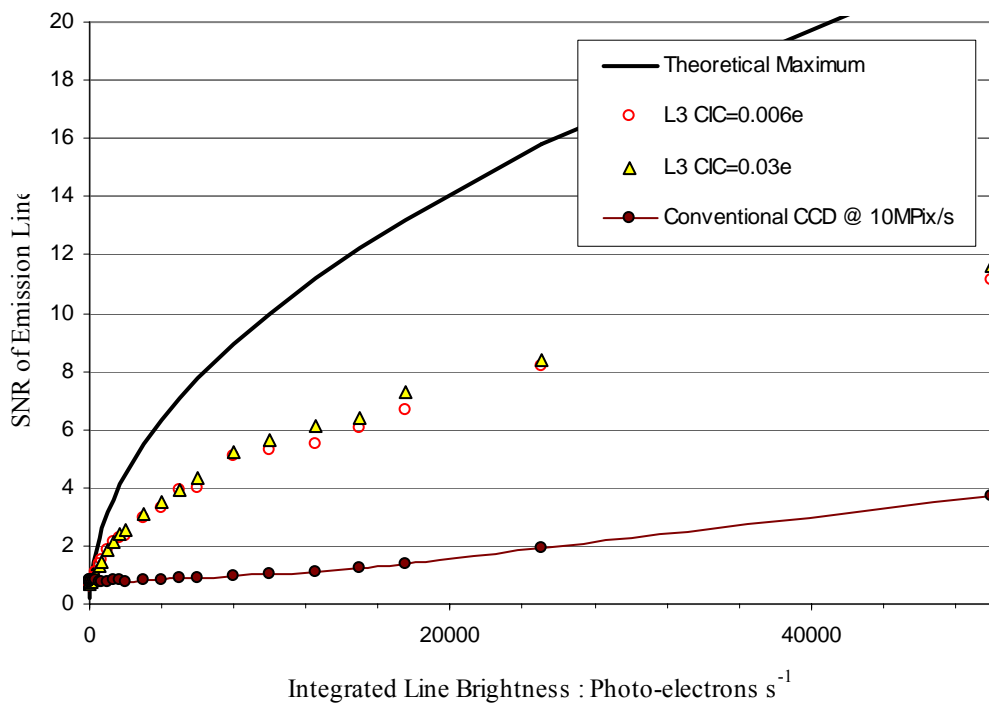


FIGURE 11. Emission line measurement: 100 Spectra s^{-1} data rate

When deciding on the photon counting threshold one should bear in mind that it should be set well below the $1e^-$ level referenced to the input of the multiplication register. In fact if it is set at exactly $1e^-$ then only 37% of the photons will be detected. To catch 90% of the photons we must use a threshold of $0.1e^-$. At the same time the threshold must not dip into the Gaussian noise of the output amplifier, small as it is, or we will measure false detections. The gain of an L3 system can be measured from a histogram of the CIC events in a bias frame or from a bias strip located within the actual spectral image. When plotted with a \log_e vertical scale, the gain, measured in ADU per photo-electron, is simply $-1 \times$ gradient. This information which is effectively embedded within the statistics of each frame can then be used to tune the threshold level. In this study a threshold of $0.15e^-$ was chosen, sufficient to catch 86% of the photo-electrons

CONCLUSIONS

For wavefront sensing the L3 detector seems to be an obvious choice. This is a very high frame rate application that is traditionally limited by detector noise and an L3 CCD allows us to get within a factor of 1.5 of the theoretical minimum centroiding noise. L3 also has the advantage of ‘failing gracefully’ at lower signal levels. In the case of conventional CCDs the centroiding fails suddenly as the guide star fades below the threshold of the algorithm. At higher exposures L3s perform worse. WFS is always photon starved however and anyway the loss is tiny: for example with an exposure of $5000e^-$ the L3 gives a centroiding noise of 0.028 pixels, the conventional CCD with $5e^-$ noise gives 0.023 pixels. The CIC would seem to be unimportant for centroiding accuracy, even at the high levels used in the model.

For spectroscopy, L3 technology can also offer significant gains if used in proportional mode. It would seem to be unbeatable at multi-Hz frame rates.

Photon counting mode is less useful for a number of reasons. Firstly it is restricted to a narrow region of operation. At the upper limit we have coincidence losses that act as a ‘brick wall’ to the signal. Not only do these losses decimate the sensitivity, they also distort the shape of the spectral lines, although in a way that should be partially correctable through an extra layer of data-reduction. At the lower limit we have CIC, amplified by the effects of image blocking and binning. For example, if we need to produce 1 spectra s^{-1} we can block 100 photon counted frames or we can take a single 1s exposure with a conventional CCD. They will produce the same SNR assuming the $CIC=0.03e^- \text{ pixel}^{-1}$ (in fact we would do much better to operate the L3 device in proportional mode). If the CIC drops further to the minimum levels quoted by the manufacturer then photon counting will do considerably better but still only marginally better than an L3 CCD operated in proportional mode and even then the improvement is only visible over a narrow range of exposure levels before coincidence losses appear.

Further models will be used to assess L3 observations of absorption lines and emission lines containing an underlying continuum. Since this moves us closer to the photon noise dominated regime it would seem reasonable to assume that the effects of multiplication noise (which acts to effectively magnify the photon noise) will further reduce the advantages of using an L3 detector.

The best all-round solution for spectroscopy would be an L3 detector that had an ultra low noise ($2.2e^- @ 100 \text{ kPix s}^{-1}$) low speed conventional amplifier at one end of its serial register for high signal/low frame rate applications and an L3 multiplication register feeding into a high speed amplifier at the other end. Signal charge would then be directed to separate amplifiers depending on the application. This is the geometry adopted by E2V for their CCD201 L3 CCD. In order to beat down CIC and permit photon counting (and at the same time boost frame rate) it would also be desirable to minimize the vertical extent of the imaging area (since CIC is proportional to the number of vertical transfers experienced by a pixel). For some applications a tall image area could still be useful so the following flexible architecture is proposed (Figure 12). If a narrow window was acceptable then it could offer an order of magnitude reduction in CIC and make photon counting more attractive.

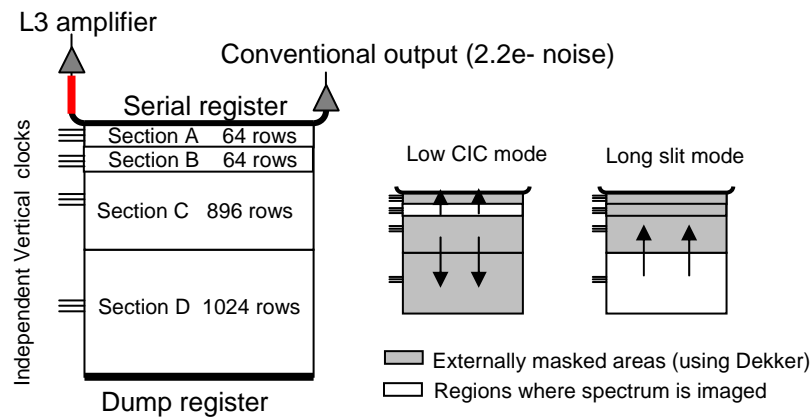


FIGURE 12. Proposed low CIC architecture

ACKNOWLEDGMENTS

Thanks to Dr. Dan Bramich (ING) for his help with the IDL programming and statistics, Dr. Jure Skvarč (ING) for advising on the centroiding algorithms and Dr. Paul Jorden (E2V) for supplying the noise data.

REFERENCES

1. E2V Technologies CCD231 Data Sheet
2. Basden, A.G., Haniff, C.A., Mackay, C.D. 2003, MNRAS 345, 985. Photon counting strategies with low-light-level CCDs (7a).
3. B.Burke, Dynamic Suppression of Interface State Dark Current in Buried Channel CCDs, IEEE Transactions on Electron Devices. Vol 38, No2 , 1991
4. J.R.Janesick, *Scientific Charge Coupled Devices*, SPIE Press, 2001, pp649
5. E2V Technologies Low Light Technical Note 4 : Dark Signal and CIC in L3 Vision CCD Sensors
6. S.Thomas,T.Fusco,Tokovinin,Nicolle,Michau,Rousset,Comparison of Centroid Computation Algorithms in a Shack-Hartmann Sensor. MNRAS. MN-06-0231-MJ.R1 200